

Modeling of Ferrofluid Passive Cooling System

Mengfei Yang^{*,1,2}, Robert O'Handley² and Zhao Fang^{2,3}

¹M.I.T., ²Ferro Solutions, Inc, ³Penn. State Univ.

*500 Memorial Dr, Cambridge, MA 02139, mengfeiy@mit.edu

Abstract: The simplicity of a ferrofluid-based passive cooling system makes it an appealing option for devices with limited space or other physical constraints. The cooling system consists of a permanent magnet and a ferrofluid. Ferrofluids are composed of nanoscale ferromagnetic particles with a temperature-dependant magnetization suspended in a liquid solvent. The cool, magnetic ferrofluid near the heat sink is attracted toward a magnet positioned near the heat source, thereby displacing the hot, paramagnetic ferrofluid near the heat source and setting up convective cooling. This paper explores how COMSOL Multiphysics can be used to model a simple cylinder representation of such a cooling system. Numerical results from the model displayed the same trends as empirical data from experiments conducted on the cylinder cooling system. These results encourage refinement of the model to more closely resemble the system and use it for designing devices and optimizing parameters.

Keywords: Navier-Stokes, ferrofluid, passive cooling, heat transfer

1. Introduction

A ferrofluid contains nanoscale ferromagnetic particles suspended in a carrier liquid. It is used in some high-power acoustic speakers to cool the drive coil. The ferromagnetic particles far from the heat source are attracted by the drive coil's magnetic field. As the fluid approaches the heat source, its temperature rises, causing the nanoparticles (with appropriate Curie temperature) to become paramagnetic. Cooler magnetic fluid near the heat sink displaces the hot paramagnetic fluid near the heat source, setting up a simple convective cooling system that fits within the confines of the device.

Modeling such systems is challenging because it involves fluid dynamics, thermal boundary conditions, and temperature-dependent magnetic properties. COMSOL Multiphysics is an ideal tool that provides rich insight into the system's behavior. The approach

was to develop a model that supports results from experiments conducted on a cylindrical container of ferrofluid with a heat source and sink [Figure 1].

The experiments involved changing the volume of the ferrofluid and moving the magnet to different positions outside the ferrofluid container. These experiments tested 1) the effect of bringing the heat source and heat sink closer together and using less ferrofluid, and 2) the optimal position for the permanent magnet between the heat source and sink. In the model, temperature-dependent magnetic properties were incorporated into the force component of the momentum equation, which was coupled to the heat transfer module. The model was compared with experimental results for steady-state temperature trends and for appropriate velocity fields. Model calculations showed that the greatest force acted along the axis of the dipole field and that the magnet is best placed midway between the heat source and sink.

2. Governing Equations

We analyze the system at steady state. The approach is to solve the heat equation and the momentum equation simultaneously to calculate the velocity vector and temperature. In this approach, the temperature-dependant magnetism of the ferromagnetic particles is included as part of the volume force in the momentum equation, so an additional magnetostatics equation is not necessary.

2.2 Heat Equation

Heat is transferred by conduction and convection in the ferrofluid. A general heat equation based on the principle of conservation of energy, which incorporates the various energy/terms, is given by

$$\rho C_p (\mathbf{u} \cdot \nabla) T = -(\nabla \cdot \mathbf{q}) + \boldsymbol{\tau} : \mathbf{S} - \frac{T}{\rho} \frac{\partial \rho}{\partial T} \left(\frac{\partial p}{\partial t} + (\mathbf{u} \cdot \nabla) p \right) + \mathbf{Q} \quad (1)$$

(See appendix for description of symbols.)

The first two terms in the equation make up the convection-diffusion equation. The third term takes into account viscous heating, the fourth term is pressure work, and the last term represents volumetric heat sources other than the ones previously mentioned.

2.3 Momentum Equation

This model assumed that the ferrofluid is an incompressible laminar fluid that obeys the Navier-Stokes equation

$$\rho \mathbf{v} \cdot \nabla \mathbf{v} = -\nabla p + \eta \nabla^2 \mathbf{v} + \mathbf{f} \quad (2)$$

(See appendix for description of symbols.)

The first term is convective acceleration. The second and third terms make up the divergence of stress, owing to pressure and viscosity, respectively. The final term is other body forces. In this model, the only other body force is from the permanent magnet, calculated in the next section using the magnetic dipole field and the ferrofluids' magnetization. If no magnet is present, then $\mathbf{f} = \mathbf{0}$.

2.4 Magnetic Force

In its most general form, force per volume is the gradient of an energy density. For the purposes of our system, which consists of a permanent magnet and ferromagnetic particles, the energy density is $\mathbf{M} \cdot \mathbf{B}$, so the force per volume is $\mathbf{F} = \nabla \mathbf{M} \cdot \mathbf{B}$.

\mathbf{B} is well approximated by the magnetic dipole field of the permanent magnet. We assume that the ferrofluids do not affect the \mathbf{B} field because of their small magnetization density and low volume concentration. In Cartesian coordinates, the three components of \mathbf{B} for a magnet pointing along the x-axis are given below

$$B_x(x, y, z) = \frac{\mu_0}{4\pi} 3\mu \frac{xz}{(x^2 + y^2 + z^2)^{\frac{5}{2}}} \quad (3)$$

$$B_y(x, y, z) = \frac{\mu_0}{4\pi} 3\mu \frac{yz}{(x^2 + y^2 + z^2)^{\frac{5}{2}}} \quad (4)$$

$$B_z(x, y, z) = \frac{\mu_0}{4\pi} 3\mu \frac{z^2 - \frac{1}{3}(x^2 + y^2 + z^2)}{(x^2 + y^2 + z^2)^{\frac{5}{2}}} \quad (5)$$

We assume that the magnitude of \mathbf{M} is only temperature dependant and that the vector points in the same direction as \mathbf{B} in all coordinates. Therefore, \mathbf{M} takes the form

$$\mathbf{M} = M(T) \cdot \mathbf{B} / \|\mathbf{B}\| \quad (6)$$

$$M(T) = 3 \cdot 10^5 \exp\{-[(T-250)/40]^6\} \quad (7)$$

Eq. 7 is not based on empirical data; the equation was chosen because it is a reasonable approximation within our range of interest (273 to ~400 K).

In other writings on this topic^{3,4}, the equation used for the force per volume is $\mathbf{F} = (\mathbf{M} \cdot \nabla) \mathbf{B}$. However, this equation does not account for the position dependence of \mathbf{M} and therefore we do not use it.

3. Experiment Method

Two experiments were conducted. In experiment 1, the steady state temperature at the heat source was measured using two different volumes of ferrofluid. For both volumes, the magnet position stayed the same distance from the heat source, but the distances between the heat source and sink were different. In experiment 2, the distance between the heat source and sink stayed the same, but the magnet's position was varied between the heat source and sink to determine optimum position for cooling.

3.1 Experiment setup

A custom-formulated ferrofluid is placed in a glass cylindrical container of 2 cm radius and ~12 cm height. The bottom of the container is sealed to a large slab of metal, acting as a heat sink at ~ 298 K. The top of the container is open to surroundings. A resistor connected to a power supply is placed near the top of the ferrofluid, providing a 10 W heat source. The permanent magnet has dimensions $1 \times 1 \times 2.6 \text{ cm}^3$ [Figure 1].

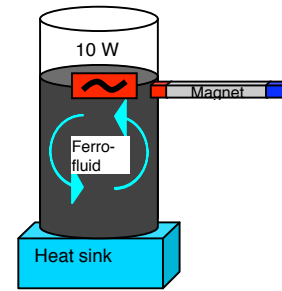


Figure 1. Setup for experiments conducted on a cylindrical container of ferrofluid.

3.2 Experiment 1

The magnet is placed in radial orientation (pointing into the axis of the cylinder, see Figure 1) along the side of the cylinder, 2 cm below the top surface of the ferrofluid. The height of the ferrofluid in the cylinder is either 5 cm or 8 cm. In each case, the power is turned on with the magnet in place. The temperature is recorded as the system comes to steady state. At steady state, the magnet is removed and temperature change is recorded. The system is allowed to reach steady state before replacing the magnet in the same position as before. Again, the temperature was recorded as the system comes to steady state. The experiment was conducted in a fume hood with airflow at about 80 fpm.

3.3 Experiment 2

The height of the ferrofluid in the cylinder was 5 cm. The magnet is initially placed in a radial orientation along the side of the cylinder at the top surface of the ferrofluid with the power on [Figure 1]. Once the system reaches steady state, the magnet is shifted lower, and the system is allowed again to reach steady state. This is repeated several times, with the magnet further lowered each time and the system allowed to reach equilibrium. The experiment was conducted in a fume hood with airflow at about 80 fpm.

4. Use of COMSOL Multiphysics

COMSOL 4.0a was used to develop a model of the cylinder cooling system described in the experiment setup section above. Two main objectives for modeling the system are 1) to accurately predict trends when parameters are varied and 2) to make design decisions that optimize the cooling system. The model that we developed in COMSOL was used to study the temperature profile and velocity flow profile of the system. It was also evaluated for how well it met the two modeling objectives by comparing the numerical results from the model with empirical data from the experiments.

The following table describes the values of the parameters used in the model.

Table 1.

Ferrofluid Parameter	Quantity
Density, ρ	1050 [kg/m ³]
Viscosity, η	0.5 [Pa*s]
Specific heat, C_p	4.2e3 [J/(kg*K)]
Thermal conductivity, K_c	0.6 [W/(m*k)]

The body force calculated in the governing equations section was for a permanent magnet located at (0,0,0) and pointing along the x-axis. Therefore, to model the radial orientation of the magnet, the axis of the cylindrical container pointed along the z-axis located on the xy-plane at (2, 0). The radius of cylinder was 2 cm, and the cylinder extended along the negative z-axis.

Two multiphysics modules were used in the modeling: Laminar Flow (single phase flow) and Heat Transfer in Fluids. Velocity and temperature variables were appropriately coupled between the two modules. The heat transfer boundary conditions were 1) 8 kW/m² boundary heat source at the top surface, 2) constant temperature at the bottom surface (298 K), and 3) heat flux from the side and top of the cylinder at a rate of 7.8 W/m²K to an ambient temperature of 298 K. The momentum boundary condition was no slip at all boundaries.

5. Experimental Results and Discussion

5.1 Experiment 1 Results

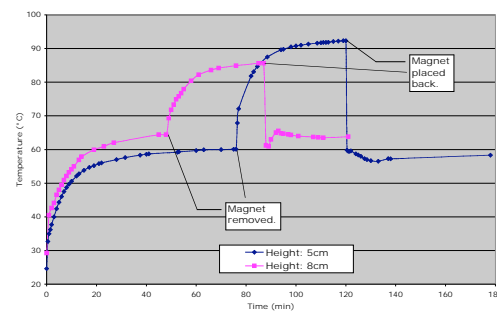


Figure 2. Comparison of steady state temperatures with and without a permanent magnet between a cylinder filled to 5 cm with ferrofluid and one filled to 8 cm with ferrofluid.

The steady state temperature was about 5°C lower in the cylinder with less ferrofluid. This extra cooling is partially due to the increased

conduction between the heat source and heat sink given the distance has decreased from 8 to 5 cm. However, the extra cooling may also be from a more optimal aspect ratio in the cylinder's geometry.

5.2 Experiment 2 Results

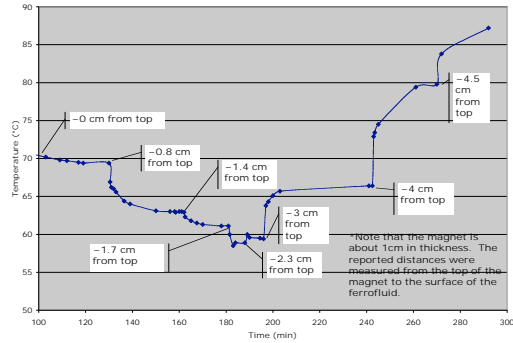


Figure 3. Steady state temperature vs. magnet position between the heat source and sink. Ferrofluid height is 5 cm.

Optimal magnet position is 1.7-2.3 cm from the top surface of the ferrofluid when the ferrofluid height is 5 cm. This is a little less than half way between the heat source and heat sink. Such a positioning might be optimal because in this region, the ferroparticles have the greatest magnetic susceptibility (they are cool enough to be magnetic). If the magnet is placed lower, it is too close to the heat sink and does not set up a large enough convective flow. If the magnet is placed higher, it is too close to the heat source where the ferrofluid is hot and the particles are paramagnetic. The data also shows that if the magnet is moved below the optimal distance, then the temperature increases more drastically than the initial temperature drop.

6. COMSOL Model and Results

Fig. 4 shows examples of the force field, velocity field, and temperature profile calculated by the model. While the quantitative values are most likely not accurate because the parameters used in the model were not based on empirical data, qualitatively, the results look reasonable. This is promising in terms of how well the model captures the physics of the system.

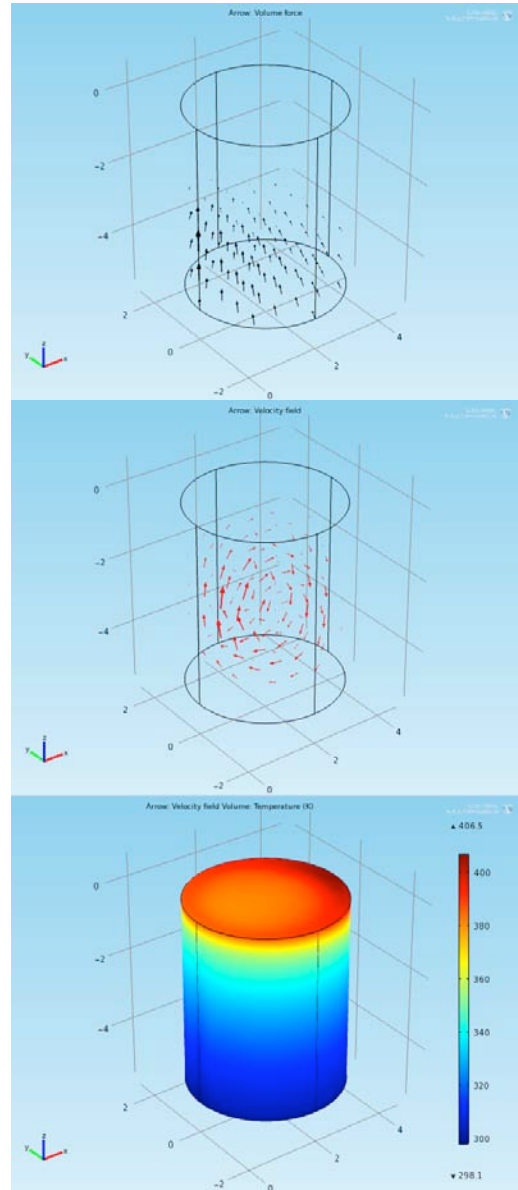


Figure 4. An example of the calculated force field, velocity field, and temperature profile of the cylinder cooling system with a magnet placed at (0,0,0) pointed in a radial orientation.

One of the trends we studied is how the maximum steady state temperature in the system varied as the distance between the heat source and heat sink changed. While we expect the temperature to decrease as the distance between source and sink decreases, owing to increasing conduction, we want to know if there is an optimal aspect ratio that maximizes the effect of

convection. Hence we compared the trend when a magnet is placed near the heat source (setting up convection as well as conduction) and when there is no magnet (purely conduction).

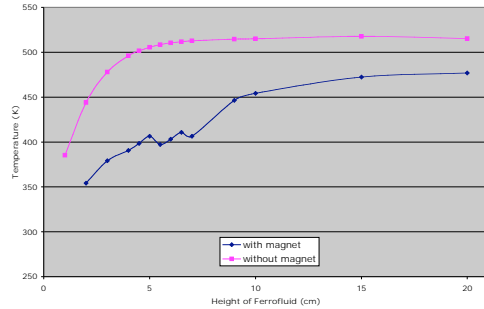


Figure 7. Magenta data set plots the dependence of the maximum steady state temperature in the system without a magnet on ferrofluid height. Blue data set represents maximum steady state temperature in the system with a magnet placed at the top surface along the side of the cylinder, pointing in radial orientation, with varying amounts of ferrofluid.

As expected, the presence of a magnet lowers the maximum steady state temperature. However, the curve does not follow the curve of the data set obtained for without a magnet. This suggests that the aspect ratio of the cylinder affects how well the magnet can set up convective flow. For example, from the model, the additional cooling owing to the magnet is much greater when the ferrofluid is at a height of 3-8 cm. When the ferrofluid height is much greater or much smaller, convective cooling is not optimized, and conduction has more effect. This can also be seen in the temperature profiles below. At 2 and 10 cm, the temperature profiles with a magnet look similar to those without a magnet. At 6 cm, the temperature profile indicates additional thermal convection.

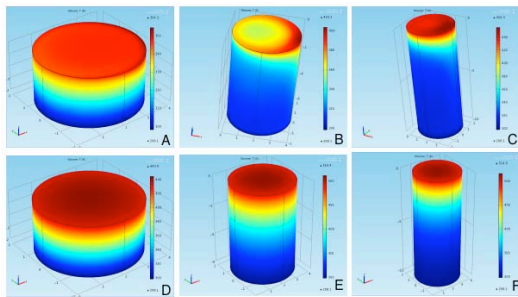


Figure 8. A-C show temperature profile of the system with 2, 6, and 10 cm, respectively, of ferrofluid when a magnet is positioned at the top surface along the side, pointing in radial orientation. D-F show the same systems as A-C except there is no magnet.

Another trend studied was how changing the magnet's position between the heat source and sink affected the maximum steady state temperature of the system. As Fig. 8 shows, the numerical model indicates the same trend as experimental results (the existence of a minimum at about half way between the heat source and heat sink). However, the numerical model showed a much greater temperature increase than was observed in experiments as the magnet is placed farther from the heat source. Thus, while the model is able to determine trends, it is quantitatively inaccurate at this stage. The model may be improved if we better understand the physics of the system and determine more accurately its physical properties.

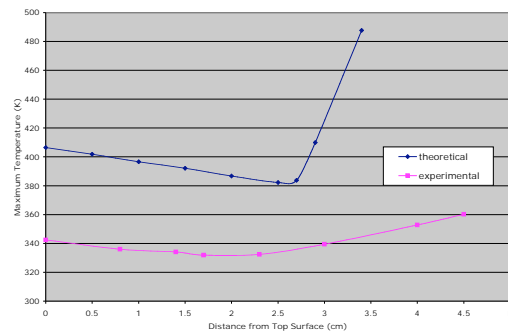


Figure 9. The blue data set represents numerical results from the COMSOL model for varying the magnet position between the heat source and sink. The height of the ferrofluid is 5 cm. The magenta data set is from experiment 2.

7. Conclusions

Through experiments, we were able to obtain empirical data of how the position of the permanent magnet and the volume of ferrofluid affect the steady state temperature of the heat source. This empirical data allowed us to determine trends that helped direct a more accurate and useful model.

The COMSOL model was able to calculate reasonable velocity fields, forces, and temperature profiles. It also qualitatively showed the same trends as those determined

from the experiments, even though there were quantitative inaccuracies. Overall, the steady state temperature decreases as the heat source is placed closer to the heat sink owing to increased conduction; however, there seems to be an optimal aspect ratio range (when the height and diameter of the cylinder are of similar lengths) where convection effects are optimized. Also, placing the magnet about halfway between the heat source and heat sink maximizes cooling.

As we understand more about the physics of the problem and gather more empirical data on its physical properties, the model will be a better representation of the system and even more useful as a predictive and designing tool.

8. References

1. Raj et al, Ferrofluid-Cooled Electromagnetic Device and Improved Cooling Method, USP Number: 5462685 (1995).
2. S. Tatarunis, and Mike Klasco, Ferrofluids, *Voice Coil* (2009).
3. T. Streck, Finite Element Simulation of Heat Transfer in Ferrofluid. InTech: Austria (2008).
4. T. Streck, Ferrofluid channel flow under the influence of magnetic dipole, *International Journal of Applied Mechanics and Engineering*, **10**, 103 (2005)

8. Appendix

Symbols used in the paper.

Symbol	Description
p	Pressure [Pa]
η	Dynamic viscosity [Pa*s]
ρ	Density [kg/m ³]
C_p	Specific heat capacity at constant pressure [J/(kg*K)]
T	Absolute temperature [K]
\mathbf{u}	Velocity vector [m/s]
\mathbf{q}	Heat flux [W/m ²]
$\boldsymbol{\tau}$	Viscous stress tensor [Pa]
\mathbf{S}	Strain rate tensor [1/s]
\mathbf{Q}	Heat source [W/m ³]
\mathbf{f}	Volume force vector [N/m ³]
K_c	Thermal conductivity [W/(m*K)]
μ	Magnetic moment [m ² A]
μ_0	Permeability constant [H/m]